

RESEARCH ARTICLE

Assessing mechanisms of climate change impact on the upland forest water balance of the Willamette River Basin, Oregon

David P. Turner^{1*} | David R. Conklin² | Kellie B. Vache³ | Cynthia Schwartz³ | Anne W. Nolin⁴ | Heejun Chang⁵ | Eric Watson⁵ | John P. Bolte³

¹Department of Forest Ecosystems and Society, Oregon State University, Corvallis, Oregon 97331, USA

²Oregon Freshwater Simulations, Portland, Oregon 97213, USA

³Department of Biological and Ecological Engineering, Oregon State University, Corvallis, Oregon 97331, USA

⁴College of Earth, Ocean, and Atmospheric Sciences, Oregon State University, Corvallis, Oregon 97331, USA

⁵Department of Geography, Portland State University, Portland, Oregon 97201, USA

Correspondence

David Turner, Department of Forest Ecosystems and Society, Oregon State University, Corvallis, Oregon 97331, USA.
Email: david.turner@oregonstate.edu

Abstract

Projected changes in air temperature, precipitation, and vapor pressure for the Willamette River Basin (Oregon, USA) over the next century will have significant impacts on the river basin water balance, notably on the amount of evapotranspiration (ET). Mechanisms of impact on ET will be both direct and indirect, but there is limited understanding of their absolute and relative magnitudes. Here, we developed a spatially explicit, daily time-step, modeling infrastructure to simulate the basin-wide water balance that accounts for meteorological influences, as well as effects mediated by changing vegetation cover type, leaf area, and ecophysiology. Three CMIP5 climate scenarios (Lowclim, Reference, and HighClim) were run for the 2010–2100 period. Besides warmer temperatures, the climate scenarios were characterized by wetter winters and increasing vapor pressure deficits. In the mid-range Reference scenario, our landscape simulation model (Envision) projected a continuation of forest cover on the uplands but a threefold increase in area burned per year. A decline (12–30%) in basin-wide mean leaf area index (LAI) in forests was projected in all scenarios. The lower LAIs drove a corresponding decline in ET. In a sensitivity test, the effect of increasing CO₂ on stomatal conductance induced a further substantial decrease (11–18%) in basin-wide mean ET. The net effect of decreases in ET and increases in winter precipitation was an increase in annual streamflow. These results support the inclusion of changes in land cover, land use, LAI, and ecophysiology in efforts to anticipate impacts of climate change on basin-scale water balances.

KEYWORDS

climate change, evapotranspiration, forest, hydrologic model, Oregon, water balance, Willamette River Basin

1 | INTRODUCTION

In forested catchments, the magnitude of evapotranspiration (ET) is often a large proportion of precipitation (Chang, Johnson, Hinkley, & Jung, 2014) and thus is a significant control on delivery of water as streamflow for human purposes. Climate change is expected to alter ET in complex ways, notably by increasing the evaporative demand of the atmosphere, influencing the characteristics of the precipitation, and changing the vegetation. Distributed hydrologic models offer the opportunity to examine potential impacts of climate change on upland forest ET, but commonly, they do not account for changing vegetation (e.g., Tohver, Hamlet, & Lee, 2014). Here, we couple a fine spatial resolution landscape simulation model (that treats changes in land cover, land use, and leaf area), with a process-based, spatially distributed

hydrology model. This combination permits assessment of multiple interacting mechanisms by which climate change might impact ET and streamflow.

The importance of vegetation changes (principally associated with disturbances) to ET and streamflow has been documented in the context of harvesting (Abdelnour, Stieglitz, Pan, & McKane, 2012), wildfire and prescribed burns (Stoof *et al.*, 2012), and insect outbreaks (Bearup, Maxwell, Clow, & McCray, 2014). Generally, a reduction in leaf area index (LAI) results in an increase in streamflow. Mechanisms accounting for that increase include reduction of transpiration, reduction in evaporation of canopy-intercepted rain, and reduction in sublimation of canopy-intercepted snow (Bearup *et al.*, 2014, Chen *et al.*, 2015, Nanko, Onda, Kato, & Gomi, 2015). More subtle changes in vegetation, as in reduction of stomatal density (and conductance) in response to

the ongoing rise in atmospheric CO₂, are also likely influencing current ET (Keenan *et al.*, 2013). Climate change is widely expected to alter the disturbance regime in the future (Dale *et al.*, 2001), and the CO₂ concentration is likely to continue rising throughout this century; thus, evaluation of climate change impacts on the hydrologic cycle should ideally consider vegetation changes as well as changes in the physical climate and CO₂ concentration (Liu, Adam, & Hamlet, 2013).

Our study area is the Willamette River Basin (WRB) in western Oregon, USA (29,728 km²). The uplands are mostly forested, but there has been a complex history in terms of ownership, management, and disturbance regime (Garman, Swanson, & Spies, 1999). The valley bottom is home to 2.6 million people and is associated with extensive non-irrigated and irrigated cropland. Urban water demand may grow significantly in the 21st century as population increases, and water supply will likely be influenced by changing climate and upland forest water fluxes.

2 | METHODS

2.1 | Overview

This study was a component of the Willamette Water 2100 project (WW2100, 2015), which was designed to simulate the water balance of the WRB as it might respond to climate and land use change over the course of the 21st century. Three recent climate scenarios, downscaled to a 4-km spatial resolution, were evaluated. We used a polygon-based landscape simulation model (Envision) to annually update the land cover and LAI, as impacted by land use change as well as disturbances (forest harvest and wildfire). A daily-time-step, spatially-distributed, hydrology model accounted for key hydrologic processes including rainfall, snowfall, canopy rain evaporation, canopy snow sublimation, transpiration, infiltration, and runoff. Results here focus on ET over the upland forest portion of the WRB, which represents 70% of its total area.

2.2 | Climate scenarios

CMIP5 results from three general circulation models (Table 1 and Figure 1) were used to represent a range of possible future climates. The selection of models was informed by an evaluation of CMIP5 model performance with respect to historical climate in the Pacific Northwest region (Rupp, Abatzoglou, Hegewisch, & Mote, 2013, WW2100, 2015). Over the range of models (LowClim, Reference, and HighClim), mean annual temperature increased between 1.2 and 5.3 °C, and annual precipitation was about the same (LowClim) or increased slightly (1–4%). Winter precipitation consistently increased

TABLE 1 Characteristics of climate scenarios.

GCM Name	RCP	Δ MAT (annual) °C	Δ P (annual) % (mm)	Δ P (JJA) % (mm)	Δ P (JFM) % (mm)	Acronym
GFDL-ESM2M	4.5	1.2	0 (0)	-15 (-15)	9 (49)	LowClim
MIROC5	8.5	3.6	4 (66)	5 (5)	13 (71)	Reference
HadGEM2-ES	8.5	5.3	1 (17)	-3 (-3)	8 (44)	HighClim

Values are changes over western Oregon (1970–1999 to 2069–2098). GCM = General Circulation Model. RCP = Representative Concentration Pathway. MAT = Mean Annual Temperature. P = Annual Precipitation.

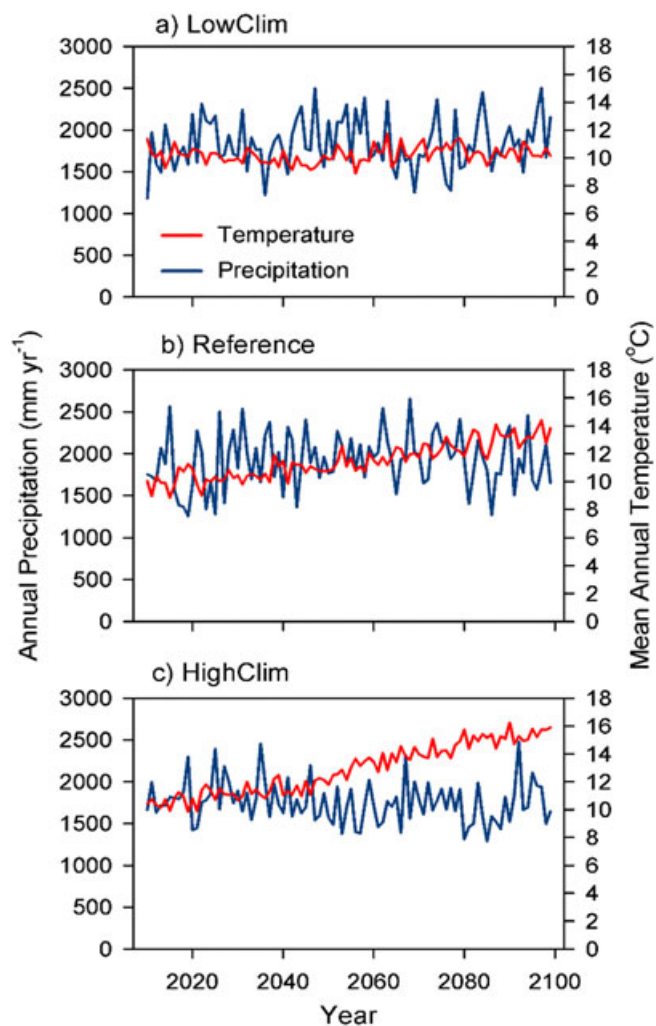


FIGURE 1 Times series (2010–2100) of annual precipitation and mean annual temperature over the Willamette River Basin for three climate scenarios

(8–13%), but summer precipitation decreased (3–15% for Highclim and LowClim, respectively) or increased (5% for Reference). The fine temporal resolution of the climate models (<1 hr) was aggregated to a daily climate data set, and the coarse spatial resolution climate model results were then downscaled to the 4-km resolution using the multi-variate adaptive constructed analogs approach (Abatzoglou & Brown, 2011). The key daily climate variables were solar radiation, precipitation, maximum temperature, minimum temperature, vapor pressure, and wind speed.

2.3 | The landscape simulator

The Envision modeling framework (Envision, 2014) was used to simulate annual changes in land cover, vegetation type, and LAI (Turner *et al.* 2015a). Envision relies on a set of state and transition models for each possible vegetation type. The typical sequence of states for a forest state and transition model is from young to mature states differing in age class and LAI. A disturbance, such as harvesting, can reset the successional stage, and vegetation type can shift at that point to an alternative cover type (based on offline runs of the MC2 dynamic global vegetation model; Rogers *et al.*, 2011) if climate has changed.

Initial conditions for land cover class, vegetation type, and stand age (if forest) were from Landsat observations, which established a network of management-level polygons (integrated decisions units, IDUs). Polygons were an average size of approximately 20 hectares. The initial rates of forest harvest and wildfire were prescribed based on Landsat observations in recent decades. Future rates of harvest depended on availability of harvest age stands, and future rates of fire were based on the offline runs of MC2, which has a fire module (Rogers *et al.*, 2011).

We assigned a representative LAI to each forest state (i.e., combination of forest type and stand age class) based on offline runs of the Biome-BGC productivity model (Thornton *et al.*, 2002) at WRB sites representative of the different forest types. Biome-BGC is prognostic with respect to LAI and has been run extensively in the Pacific Northwest to simulate forest growth (Turner *et al.*, 2011). A 25-year daily climate data set from ORNL (2014) was used to initialize the model and run from stand replacing disturbance through the complete range of stand ages. In the Biome-BGC simulations, LAI ranged between 0 and 8 depending on stand age and location, consistent with observations in the region (Marshall & Waring, 1986). Maximum values were associated with older stands at low to mid-elevations.

Each forest state was also assigned a stand height for use in estimating aerodynamic resistance. Again, that was based on stand age. A reference stand age to height relationship (Equation 1) was constructed from observations of mean stand age and mean height for stands ($n = 207$) in the West Cascades ecoregion from the USDA Forest Service forest inventory and analysis data set (FIA, 2006).

$$h = 46.6 (1 - e^{-a}), \quad (1)$$

where

h mean height in meters.

a stand age in years.

2.4 | The hydrology model

An existing watershed hydrology model (Hydrologiska Byråns Vattenbalansavdelning (HBV), Bergström & Singh, 2012) was adapted for use in the WRB. The WRB version (Willamette hydrology model) generates daily-time-step estimates for ET (transpiration + soil evaporation) based on the Penman–Monteith approach (ET_{PM}), canopy-intercepted rain evaporation (CR_e), canopy-intercepted snow sublimation (CS_s), and soil water status (SW). Units are mm or mm/day. Algorithms for key processes are as follows.

2.4.1 | Rain and snow

Precipitation (P) was partitioned into rain (R) and snow (S) based on air temperature. At or above +6 °C, all P is R ; at or below -2 °C, all P is S ; between those temperatures, P is partitioned proportionally between R and S .

2.4.2 | Canopy transpiration + soil evaporation

An initial LAI-specific potential daily ET_{PM} rate was determined based on the Penman–Monteith approach (Allen *et al.*, 2005), with inputs of solar radiation (for estimation of net short-wave radiation), air

temperature (for estimation of saturation vapor pressure and net long-wave radiation), vapor pressure (for estimation of vapor pressure deficit [VPD]), and LAI (for estimation of bulk stomatal resistance), as well as wind speed and stand height (for estimation of canopy aerodynamic resistance). Surface albedo was assumed to be 0.15 (Jarvis, 1976). Reference stomatal resistance was based on Kelliher, Leuning, and Schulze (1993).

The potential ET_{PM} was then modified by scalars (0–1) based on soil water status and VPD to determine the actual ET_{PM} , with only the lower of the two scalars applied on any given day. The soil water scalar was a linear ramp from 1 to 0 based on the ratio of current SW to available soil water (field capacity–wilting point capacity). The ramp began at 1.0 for a ratio of 0.5 and decreased to 0 at a ratio of 0. The VPD scalar is described in Equation 2.

$$VPD_{\text{scalar}} = (1 - ((VPD - VPD_{\text{min}}) / (VPD_{\text{max}} - VPD_{\text{min}}))), \quad (2)$$

where VPD_{min} (0.610 MPa) and VPD_{max} (3.100 MPa) are based on observations in coniferous forests at the leaf level (Griew, Guehl, & Aussenac, 1988) and at eddy covariance towers (Wharton, Schroeder, Bible, Falk, & Paw, 2009). VPD_{scalar} was set to 1.0 below VPD_{min} and set to a minimum of 0.02 as VPD approaches VPD_{max} . The VPD scalar accounts for the observations that conifer transpiration in the Pacific Northwest is generally sensitive to VPD (Bond & Kavanagh, 1999, Wharton *et al.*, 2009). Under low LAI conditions, aerodynamic resistance would be high, so the VPD scalar has little effect. In the Pacific Northwest summer (generally warm and dry), the litter/upper soil would be dry under high VPD conditions, and soil surface resistance would be high in any case.

An additional optional parameter was introduced as a control on stomatal resistance to evaluate potential effects of atmospheric CO_2 on transpiration. When this control was operating, the stomatal resistance was increased by 20% in a linear fashion over the CO_2 concentration range from 400 to 800 ppm (Way, Oren, & Kroner, 2015). Year-specific CO_2 concentration values were from the CMIP5 representative concentration pathways associated with the particular climate model runs we used (RCP, 2015).

2.4.3 | Canopy rain evaporation

These fluxes occur at night as well as during the day and rely in part of advected energy (Pearce, Rowe, & Stewart, 1980, Humphreys *et al.*, 2003); thus, they may not be covered by ET_{PM} . Observations at a conifer forest site in the Cascade mountains (Link, Unsworth, & Marks, 2004, Pypker, Bond, Link, Marks, & Unsworth, 2005) suggest CR_e losses of about 25% of rainfall under full canopy conditions (LAI \approx 8). CR_e has also been observed to decrease with LAI in conifer forests (Nanko *et al.*, 2015). Here, we modeled CR_e as a linearly increasing fraction of rainfall ranging from 0% to 24% over an LAI range from 0 to 8.

2.4.4 | Canopy snow sublimation

Observations of CS_s in conifer stands (Montesi, Elder, Schmidt, & Davis, 2004) suggest maximum values as a proportion of snowfall of about 20–30% with high LAI conditions. Here, we estimated CS_s as a linearly increasing fraction of snowfall ranging from 0% to 20% over an LAI range from 0 to 8. Residual snow was deposited on the ground.

The sum of ET_{PM} , CR_e , and CS_s is labeled ET_{SUM} (albeit sublimation is included).

2.4.5 | Snow melt

The snow melt and sublimation function include a temperature term and an energy term, as implemented in the Biome-BGC model (Ichii, White, Votava, Michaelis, & Nemani, 2008). The temperature term is a simple multiplicative function (as in HBV) with mean air temperature and a parameterized coefficient. In the energy term, the radiation available for snow melt is a function of the incident short-wave radiation, the short-wave radiation transmittance through the canopy (SW_t), and the absorptivity of the snow.

$$SW_t = e^{-(LAI * K)} \quad (3)$$

where LAI is LAI and K (0.5) is the extinction coefficient. Above 0 °C, the available energy is used for snow melt (latent heat of fusion = 335 kJ/kg), and below 0 °C, it is used for sublimation (latent heat of fusion = 2,835 kJ/kg). Simulated snowpack dynamics in the early years of the model runs at selected SNOTEL (2016) sites approximated long-term means from historical observations.

2.4.6 | Soil water status

The storage and release of water are captured with an approach that includes three conceptual stores representing soil, fast watershed response, and slow watershed response (Bergström & Singh, 2012). Snow melt and canopy throughfall contribute water to soil, and in increasing fractions to the fast watershed response store when the soil compartment becomes saturated. ET_{PM} is taken from the soil store. The geographic subunits in the subsurface hydrology scheme for Willamette hydrology model are termed hydrologic response units (HRUs), and all IDUs within an HRU shared the same reservoir of soil water, as in HBV. The soil water holding capacity of the HRUs was specific to the sub-basin in which it was found. These sub-basin values were from calibrations using the PEST software suite (Doherty & Johnston, 2003) and historical observations of climate and streamflow.

3 | RESULTS

Elevation in the WRB extends from 60 m at the mouth of the river in Portland to nearly 4,000 m at the top of Mount Jefferson, one of the highest remnant volcanoes in the Oregon Cascades Mountains (Figure 2a). The vegetation cover of the uplands is predominantly conifer forest (Figure 2b). Much of the upland forest is managed primarily for wood harvest; thus, there is considerable heterogeneity in stand age, and correspondingly LAI (Figure 2c). Harvests on public forestland occur at a much lower rate than on private forestland, so mean LAI is higher at the mid-elevations, which are predominantly in public ownership. Maximum LAI in high-elevation subalpine forests is lower than in mid-elevation and low elevation forests.

The geographic pattern of ET_{PM} in 2010 shows the effects of the disturbance regime, that is, low ET_{PM} at low elevations where significant areas have been recently clear-cut (Figure 3). Highest ET_{PM} is at mid-elevations, with high LAI and high precipitation. High LAI supports relatively high ET_{PM} because of the role of foliage in transpiration. At the highest elevations, ET_{PM} decreases because of lower LAI, shorter growing season, and lower soil water-holding capacity.

Basin-wide mean forest LAI shows responses to large fires in all scenarios (Figure 4). The more extreme the climate scenario, the bigger the year-to-year changes in LAI. A threefold increase in annual average burned area was simulated with the Reference scenario and a ninefold increase for the HighClim scenario. Simulated harvest rates were stable in the LowClim and Reference scenarios but were reduced on private forestland in the later part of the century in the HighClim scenario because of low availability of harvest age stands (due to fire). Basin-wide mean LAI declined between 12% and 30% over the course of the 90-year scenarios. The potential vegetation type for the forest uplands of the WRB remained as forest in all scenarios.

The water budget for the upland forests (Reference scenario) suggests an ET_{SUM} to precipitation ratio of 0.38 averaged over the 2010–2039 period (Table 2). R increased (13%), but S decreased (–45%) between 2010–2039 and 2070–2099 (Table 2). Basin-wide mean ET_{PM} and CR_e decreased slightly, and CS_s decreased substantially (–49%).

The basin-wide mean forest ET_{SUM} for all scenarios decreased (–4% to –20%) from the beginning to the end of the simulation period (Figure 5). The impact of LAI on ET_{SUM} was especially evident in the

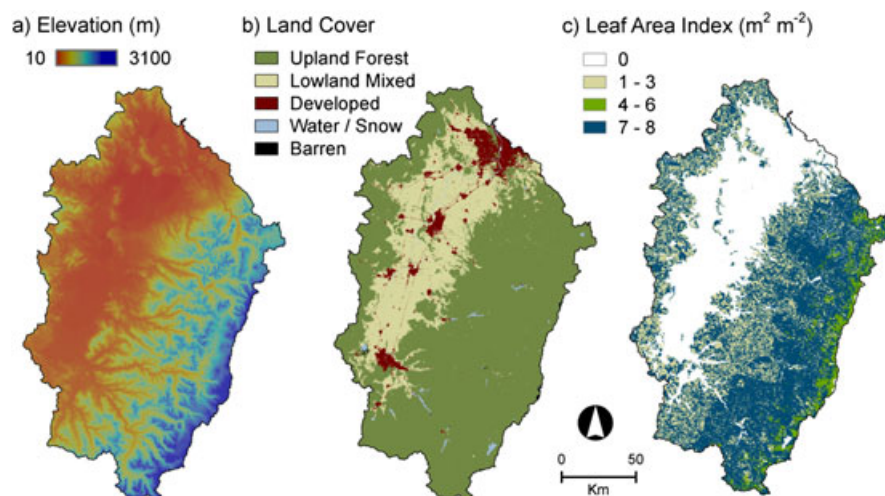


FIGURE 2 Willamette River Basin in 2010: (a) elevation, (b) land cover, and (c) leaf area index. The geographic projection is Albers

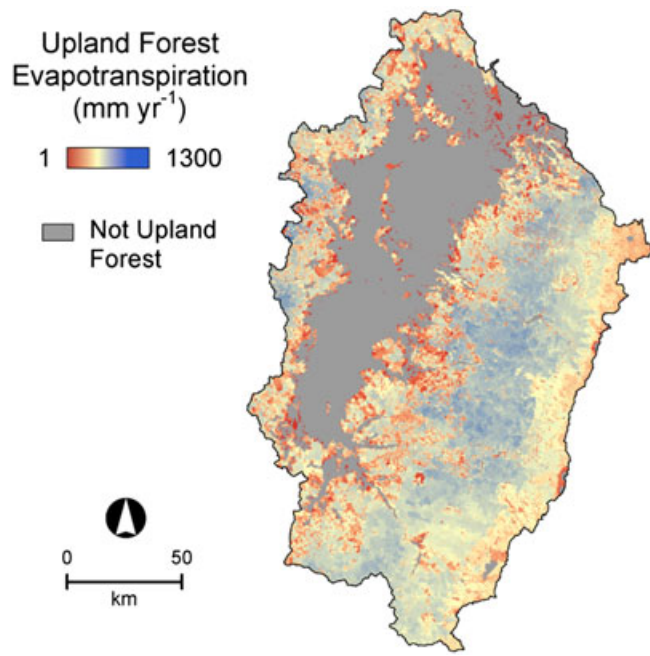


FIGURE 3 Simulated annual Penman–Monteith evapotranspiration (ET_{PM}) in the year 2010 for the upland forests of the Willamette River Basin

HighClim case where ET_{SUM} dropped appreciably in a high fire year (2053), in parallel with LAI. The driving factors for the decrease in ET_{SUM} included the influence of low LAI on ET_{PM} , CR_e , and CS_s , and the influence of the VPD (Figure 6) and soil water scalars on ET_{PM} . ET_{SUM} did increase in undisturbed forest areas at high elevation.

Model runs in which vegetation was held constant, while the VPD constraint and the soil water constraint were not imposed, suggested up to a 40% increase in evaporative demand over the course of the scenarios due exclusively to climate change (Figure 7). As noted, however, the net effect when vegetation change, the VPD constraint, and the soil water constraint were imposed was a decrease in ET_{PM} . When the effect of atmospheric CO_2 on stomatal conductance was added to the base case, ET_{PM} was further reduced (an additional -11% to -18%) by the year 2100 (Figure 8). Under the Reference scenario with the CO_2 influence operating, ET_{SUM} was reduced 18%.

These simulation results suggest a strong influence of projected climate change and CO_2 increase on WRB vegetation and water balance. Three factors will tend to reduce annual ET: (a) Increased

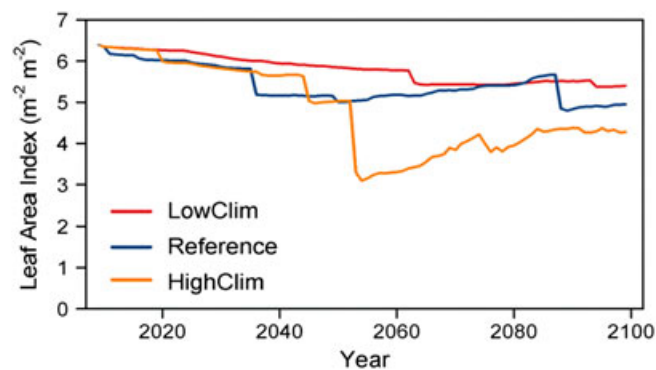


FIGURE 4 Time series of Willamette River Basin-wide (forested area) mean for leaf area index

TABLE 2 Water balance components for the upland forests (averaged overall Willamette River Basin-forested polygons)

	2010–2039	2070–2099	Change (%)
Participation	1,860	1,918	+3
Rain	1,541	1,744	+13
Snow	319	174	−45
Penmon–Monteith evapotranspiration	386	378	−2
Canopy rain evaporation	289	278	−4
Canopy snow sublimation	49	25	−49
Total evapotranspiration	711	682	−4
Residual (=streamflow)	1,149	1,236	+7

Note. Values are 30-year means for the Reference scenario. Units are mm/year.

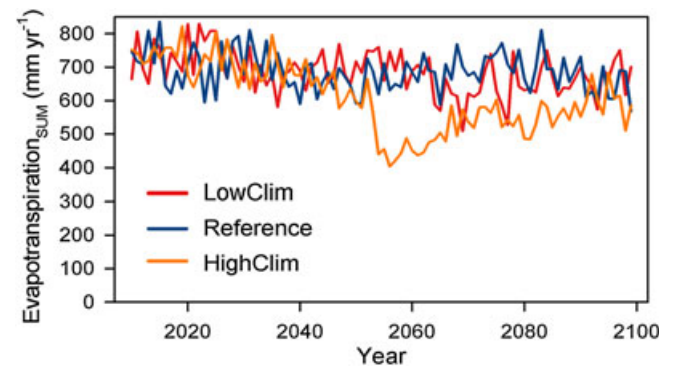


FIGURE 5 Time series of Willamette River Basin-wide (forested area) mean for annual summed evapotranspiration (ET_{SUM})

disturbance will reduce basin-wide mean LAI, (b) higher VPDs and lower soil water availability will reduce transpiration, and (c) increasing CO_2 will reduce stomatal conductance. Together, these factors will offset the effect of increasing evaporative demand on annual ET.

4 | DISCUSSION

4.1 | Near-term WRB uplands water balance

At the IDU level, our estimates of maximum daily ET_{PM} in high LAI stands were of a similar magnitude (3–5 mm/day) to estimates from conifer stands in the West Cascades ecoregion using eddy covariance towers (Unsworth *et al.*, 2004) and streamflow calibrated models (Garcia, Tague, & Choate, 2013). The annual cycle of ET_{PM} showed low values in the winter associated with low energy availability, and low values in August and September as a result of constraints imposed by VPD and soil water status. This seasonal pattern is similar to flux tower observations in the region (Humphreys *et al.*, 2003, Wharton *et al.*, 2009). Inter-annual variation in annual ET_{PM} of about 10% of the mean also corresponds to observations in other temperate conifer forests (e.g., (Thomas *et al.*, 2009)).

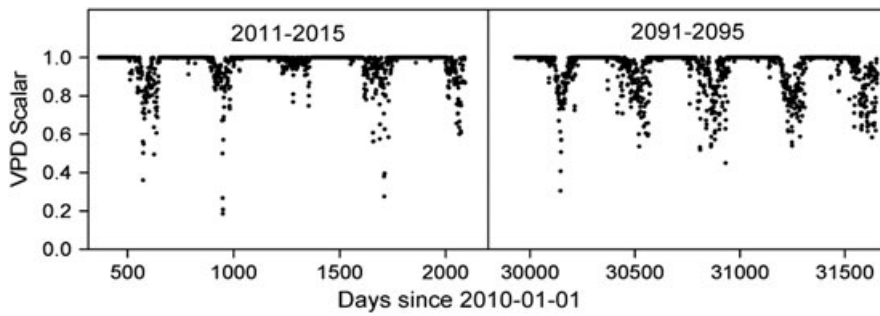


FIGURE 6 Five-year daily time series of Willamette River Basin-wide (forested area) mean vapor pressure deficit (VPD) scalar for 2011–2015 and 2091–2095

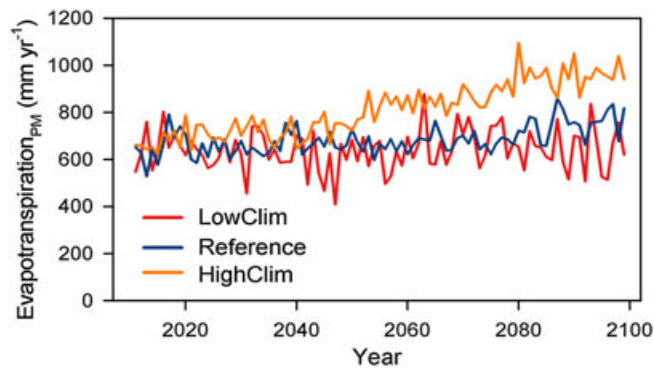


FIGURE 7 Time series of Willamette River Basin-wide (forested area) mean for Penman–Monteith evapotranspiration (ET_{PM}). Model runs were made with no vegetation change, no soil water constraint, and no vapor pressure deficit constraint

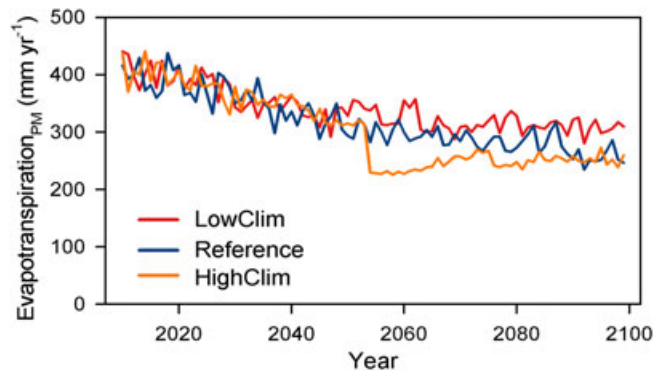


FIGURE 8 Time series of Willamette River Basin-wide (forested area) mean for Penman–Monteith evapotranspiration (ET_{PM}). Model runs allowed vegetation change, the soil water constraint, the vapor pressure deficit constraint, and the CO_2 influence on stomatal conductance

Our WRB uplands ET_{SUM} to P ratio of about 0.38 in the early years of the scenarios compares closely to the same ratio estimated from the balance of observed precipitation and streamflow for various unregulated sub-basins of the WRB (Chang *et al.*, 2014). Our CR_e to R ratio was 0.19 on an annual basis, which compares to a range of 0.10 to 0.30 for observations in conifer forests of the Pacific Northwest (Moore & Wondzell, 2005). The CS_s to S ratio (0.15) on an annual basis is consistent with canopy snow sublimation observations of about 100 mm/year in a mature Douglas-fir stand in the West Cascades ecoregion (Storck, Lettenmaier, & Bolton, 2002). Our mix of low and high LAI stands over the WRB is expected to yield lower

basin-wide mean ratios of ET_{SUM} to P , CR_e to R , and CS_s to S than would be measured in a single mature forest stand.

Soil evaporation is assumed to be covered by ET_{PM} in our modeling approach. However, litter/soil resistance is not explicitly modeled, which introduces considerable uncertainty. Soil evaporation is difficult to measure directly but is likely much lower (<0.5 mm/day) than transpiration under moderate-to-high LAI conditions (Heal, Stidson, Dickey, Cape, & Heal, 2004; Nelson, Kurc, John, Minor, & Barron-Gafford, 2014). Our LAI simulations assumed LAI recovery began the year after a disturbance, so most area generally had significant LAI. Under low LAI conditions, soil evaporation is limited in winter because of low temperature and low solar radiation. It would tend to be self-limiting in the dry summers of the Pacific Northwest because surface resistance increases with drying of the litter and upper soil layers. Optimally, an energy balance approach to simulating soil evaporation, which included surface resistance, could be employed if observations were available for calibration and validation.

The geographic pattern of our contemporary upland ET_{SUM} to P ratio is significantly affected by the pattern of LAI. Thus, areas of heavily managed forests in the lowlands tend to have lower LAIs and ET_{SUM} to P ratios than less disturbed areas at higher elevations. Note that relatively few river basin scale hydrologic simulation models account for management or climate-related variation in LAI (e.g., Tesemma, Wei, Peel, & Western, 2015). Here, we estimated LAI indirectly by way of stand age, but both satellite and airborne remote sensing have potential for mapping LAI (Livneh *et al.*, 2015) and could be used to specify initial conditions for basin-scale hydrology models.

4.2 | Projected changes in climate and vegetation

The CMIP5 climate projections out to 2100 for the WRB suggest increases in mean annual temperature. This trend would follow historic increases observed in the climate record (Liu *et al.*, 2013). Projected changes in precipitation are more equivocal but agree on increases in winter precipitation, which would correspond to the generally expected intensification of the hydrologic cycle associated with increasing greenhouse gas concentrations. With warmer temperatures, VPD increased in our projected climates, for example, from a mean May to September VPD of 0.71 MPa in the 2010s to 0.87 MPa in the 2090s in our Reference scenario, and to 1.24 MPa in the 2090s in the HighClim scenario.

Our conclusion (here and in Turner, Conklin, & Bolte, 2015a) that the uplands of the WRB will likely remain forested throughout the 21st century is in agreement with previous studies using the climate

envelope approach (Shafer, Bartlein, & Thompson, 2001) and global biogeography models (Rogers *et al.*, 2011, Shafer, Bartlein, Gray, & Pelltier, 2015). The MC2 simulations suggested a shift at low elevations towards more mixed conifer-hardwood forest types. Hardwood species tend to exhibit different stomatal conductance and sensitivity to VPD compared to conifers (Bond & Kavanagh, 1999), which could impact the seasonality and annual sum of ET.

The incidence of fire in the early decades of the simulations (0.2% of forest land area per year) was comparable to remote sensing-based observations in the West Cascades ecoregion (Turner, Conklin, & Bolte, 2015b). The projected threefold to ninefold increases in the area burned per year in the Reference and HighClim scenarios are consistent with empirical approaches to projecting burned area based on future climates and current ecoregional patterns in climate and the incidence of fire (Littell, McKenzie, Peterson, & Westerling, 2009, Dennison, Brewer, Arnold, & Moritz, 2014). Increased fire disturbance in combination with sustained rates of forest harvesting tends to reduce basin-wide mean LAI in our simulations.

4.3 | Net effects of climate change on ET and water balance

The modest decline in simulated ET_{SUM} over the course of the 21st century in our three scenarios was driven by a complex interaction of direct and indirect effects of climate change. The influence of decreasing LAI was particularly strong because reduced leaf area influenced ET_{PM} , CR_e , and CS_s . In contrast, the climate models imposed increases in winter precipitation (all scenarios) that tended to increase CR_e but did not increase CS_s because S decreased (Table 2). Higher temperatures extended the growing season, and associated increases in VPD increased ET_{PM} (when soil water was available and VPD had not begun to restrict stomatal conductance). Our results from isolating the change in evaporative demand showed greater increases in annual evaporative demand with greater increases in mean annual temperature. However, even under the current climate in the WRB, ET is often constrained in August and September by low soil moisture when evaporative demand is greatest (Runyon, Waring, Goward, & Welles, 1994); thus without an increase in summer precipitation, summer ET largely did not increase in our projections. With reference to annual streamflow, the dominant effect of increasing VPD in the future may be to induce stomatal closure earlier in the growing season, thus counteracting its tendency to increase transpiration in the spring (Tague, Heyn, & Christensen, 2009).

Our results differ from several previous assessments of climate change impacts on ET in the WRB. Jung and Chang (2011) used the Precipitation-Runoff Modeling System (PRMS) model and CMIP3 climate scenarios and reported stable ET over the course of the century. Tohver, Hamlet, and Lee (2014) used the Variable Infiltration Capacity (VIC) model and reported higher summer ET in the future. The differences between the current study and their studies are likely to result from the fact that their modeling did not account for possible changes in vegetation, as well as use of different general circulation models.

4.4 | CO₂ effect

Our simulations that include a reduction in stomatal conductance with increasing atmospheric CO₂ concentration suggest a strong additive effect on ET_{PM} reduction. However, the magnitude of changes in stomatal conductance as a function of CO₂ increase is highly uncertain. There is clear evidence in the fossil record of reduced stomatal density under high CO₂ conditions previous to the Pleistocene era (3 Mya–11 Kya), and experimental increases in atmospheric CO₂ often reduce stomatal conductance (Franks *et al.*, 2013). Also, observations at eddy covariance towers suggest an increase in water use efficiency in recent decades (Keenan *et al.*, 2013), possibly driven by the concurrent CO₂ increase. Elevated CO₂ is not expected to increase LAI in energy-limited (annual precipitation > annual potential ET) ecoregions such as the West Cascades (Norby & Zak, 2011).

The effect of CO₂ was greater in the case of representative concentration pathway 8.5 scenarios (Reference and HighClim) than with the representative concentration pathway 4.5 (LowClim) scenario because the CO₂ concentration reached much higher values (950 ppm vs. 500 ppm). Our sensitivity analysis suggests that the CO₂ constraint could largely offset the effects of increasing evaporative demand. Reduced transpiration per unit of leaf area could work in combination with reduced LAI from disturbances to produce surprisingly large decreases in ET. Considering also a projected higher winter precipitation, which would mostly go directly to streamflow (Elsner *et al.*, 2010), substantial increases in annual streamflow are possible in the WRB.

4.5 | Uncertainty issues

Our projections of future hydrologic flows are strongly dependent on multiple process-based simulation models, each with a degree of uncertainty. Innovations in the hydrologic model here—notably annual updating of LAI to account for disturbances, and factoring in the effect of CO₂ on transpiration—helped reduce uncertainty with respect to climate change impacts on forest hydrology. Hydrology model limitations include simplified treatment of soil evaporation and snowpack sublimation/evaporation. Our wind fields did not account for possible increases in wind speed associated with more open disturbed areas, which would increase both soil evaporation and snowpack water vapor flux. Observations suggest that higher snowpack sublimation/evaporation does compensate for less canopy snow sublimation in some highly disturbed mountainous regions (Biederman *et al.*, 2014, 2015).

Our dynamic global vegetation model had the benefit of linking the disturbance regime to climate change, thus adding the influence of disturbance to the hydrological modeling. Limitations included uncertainty about the fire submodel sensitivity to changes in climate, and the simple all or nothing change in LAI when a disturbance was specified. Projected climates from general circulation models also add uncertainty to both the vegetation and hydrology modeling, especially at the regional scale. Here, we evaluated multiple climate models and applied statistical downscaling to help constrain that uncertainty.

5 | SUMMARY AND CONCLUSIONS

The future climate of western Oregon is likely to be warmer, wetter in the winter, and drier in the summer. Evaluation of the potential impacts of these changes on streamflow must include accounting for possible alteration of vegetation structure and ecophysiology. Here, we constructed a basin-wide hydrology simulation framework that includes sensitivity to vegetation change and climate. In the WRB, vegetation cover is expected to remain as forests but continued harvesting, and an increased incidence of fire may reduce basin-wide mean leaf area. Decreases in LAI will likely reduce basin-wide ET because of its direct influence on ET, CR_e , and CS_s . If ET is also suppressed by high VPDs and high CO_2 , then total ET may decrease rather than increase as is projected by similar modeling exercises that do not include vegetation change. Higher winter precipitation will mostly contribute to runoff; thus, mean annual streamflow may well be considerably higher than historic levels.

ACKNOWLEDGMENTS

Thanks to John Abatzoglou (University of Idaho) for the multivariate adaptive constructed analogs downscaling, Andrew Gray (USDA Forest Service) for developing the stand age to height function, and David Ritts (Oregon State University) for creating the figures. Support was provided by the National Science Foundation under grant EAR-1039192 and EAR-1038925 to the Willamette River 2100 Project. Views expressed are our own and do not necessarily reflect those of sponsoring agencies.

REFERENCES

- Abatzoglou, J. T., & Brown, T. J. (2011). A comparison of statistical downscaling methods suited for wildfire applications. *International Journal of Climatology*, 32, 772–780.
- Abdelnour, A., Stieglitz, M., Pan, F. F., & McKane, R. (2012). Catchment hydrological responses to forest harvest amount and spatial pattern. *Water Resources Research*, 48, W03902.
- Allen, R. G., Walter, I. A., Elliot, R. L., JHowell, T. A., Itenfisu, D., Jensen, M. E., & Snyder, R. (2005). *The ASCE standardized reference evapotranspiration equation* ASCE and American Society of Civil Engineers: Report No.
- Bearup, L. A., Maxwell, R. M., Clow, D., & McCray, J. E. (2014). Hydrological effects of forest transpiration loss in bark beetle-impacted watersheds. *Nature Climate Change*, 4, 481–486.
- Biederman, J. A., Brooks, P. D., Harpold, A. A., Gochis, D. J., Gutmann, E., Reed, D. E., ... Ewers, B. E. (2014). Multiscale observations of snow accumulation and peak snowpack following widespread, insect-induced lodgepole pine mortality. *Ecohydrology*, 7, 150–162.
- Biederman, J. A., Somor, A. J., Harpold, A. A., Gutmann, E. D., Breshears, D. D., Troch, P. A., ... Brooks, P. D. (2015). Recent tree die-off has little effect on streamflow in contrast to expected increases from historical studies. *Water Resources Research*, 51, 9775–9789.
- Bergström, S., & Singh, V. P. (2012). The HBV Model. In V. P. Singh (Ed.), *Computer models of watershed hydrology*. Water Resources Publications.
- Bond, B. J., & Kavanagh, K. L. (1999). Stomatal behavior of four woody species in relation to leaf-specific hydraulic conductance and threshold water potential. *Tree Physiology*, 19, 503–510.
- Chang, H. J., Johnson, G., Hinkley, T., & Jung, I. W. (2014). Spatial analysis of annual runoff ratios and their variability across the contiguous US. *Journal of Hydrology*, 511, 387–402.
- Chen, F., Zhang, G., Barlage, M., Zhang, Y., Hicke, J. A., Meddens, A., ... Frank, J. (2015). An observational and modeling study of impacts of bark beetle-caused tree mortality on surface energy and hydrological cycles. *Journal of Hydrometeorology*, 16, 744–761.
- Dale, V. H., Joyce, L. A., McNulty, S., Neilson, R. P., Ayres, M. P., Flannigan, M. D., ... Wotton, B. M. (2001). Climate change and forest disturbances. *Bioscience*, 51, 723–734.
- Dennison, P. E., Brewer, S. C., Arnold, J. D., & Moritz, M. A. (2014). Large wildfire trends in the western United States, 1984–2011. *Geophysical Research Letters*, 41, 2928–2933.
- Doherty, J., & Johnston, J. M. (2003). Methodologies for calibration and predictive analysis of a watershed model. *Journal of the American Water Resources Association*, 39, 251–265.
- Elsner, M. M., Cuo, L., Voisin, N., Deems, J. S., Hamlet, A. F., Vano, J. A., ... Lettenmaier, D. P. (2010). Implications of 21st century climate change for the hydrology of Washington state. *Climatic Change*, 102, 225–260.
- Envision. (2014). Retrieved from: <http://envision.bioe.orst.edu/>
- FIA. (2006). U.S. Department of Agriculture Forest Inventory and Analysis Program. Retrieved from: <http://fia.fs.fed.us>
- Franks, P. J., Adams, M. A., Amthor, J. S., Barbour, M. M., Berry, J. A., Ellsworth, D. S., ... von Caemmerer, S. (2013). Sensitivity of plants to changing atmospheric CO_2 concentration: From the geological past to the next century. *New Phytologist*, 197, 1077–1094.
- Garcia, E. S., Tague, C. L., & Choate, J. S. (2013). Influence of spatial temperature estimation method in ecohydrologic modeling in the western Oregon Cascades. *Water Resources Research*, 49, 1611–1624.
- Garman, S. L., Swanson, F. J., & Spies, T. A. (1999). Past, present, future landscape patterns in the Douglas-fir region of the Pacific Northwest. In J. A. Rochelle, L. A. Lehmann, & J. Wisniewski (Eds.), *Forest fragmentation: Wildlife and management implications*. (pp. 61–86). The Netherlands: Brill Academic Publishing.
- Griew, P., Guehl, J. M., & Aussenac, G. (1988). The effects of soil and atmospheric drought on photosynthesis and stomatal control of gas-exchange in 3 coniferous species. *Physiologia Plantarum*, 73, 97–104.
- Heal, K. V., Stidson, R. T., Dickey, C. A., Cape, J. N., & Heal, M. R. (2004). New data for water losses from mature Sitka spruce plantations in temperate upland catchments. *Hydrological Sciences Journal-Journal Des Sciences Hydrologiques*, 49, 477–493.
- Humphreys, E. R., Black, T. A., Ethier, G. J., Drewitt, G. B., Spittlehouse, D. L., Jork, E. M., ... Livingston, N. J. (2003). Annual and seasonal variability of sensible and latent heat fluxes above a coastal Douglas-fir forest, British Columbia, Canada. *Agricultural and Forest Meteorology*, 115, 109–125.
- Ichii, K., White, M. A., Votava, P., Michaelis, A., & Nemani, R. R. (2008). Evaluation of snow models in terrestrial biosphere models using ground observation and satellite data: Impact on terrestrial ecosystem processes. *Hydrological Processes*, 22, 347–355.
- Jarvis, P. G. (1976). The interpretation of the variations in leaf water potential and stomatal conductance found in canopies in the field. *Philosophical Transactions of the Royal Society of London. Series B, Biological Sciences*, 273, 593–610.
- Jung, I. W., & Chang, H. J. (2011). Assessment of future runoff trends under multiple climate change scenarios in the Willamette River Basin, Oregon, USA. *Hydrological Processes*, 25, 258–277.
- Keenan, T. F., Hollinger, D. Y., Bohrer, G., Dragoni, D., Munger, J. W., Schmid, H. P., Richardson, A. D. (2013). Increase in forest water-use efficiency as atmospheric carbon dioxide concentrations rise. *Nature* 499, 324.
- Kelliher, F. M., Leuning, R., & Schulze, E. D. (1993). Evaporation and canopy characteristics of coniferous forests and grasslands. *Oecologia*, 95, 153–163.
- Link, T. E., Unsworth, M., & Marks, D. (2004). The dynamics of rainfall interception by a seasonal temperate rainforest. *Agricultural and Forest Meteorology*, 124, 171–191.
- Littell, J. S., McKenzie, D., Peterson, D. L., & Westerling, A. L. (2009). Climate and wildfire area burned in western U. S. ecoregions, 1916–2003. *Ecological Applications*, 19, 1003–1021.

- Liu, M. L., Adam, J. C., & Hamlet, A. F. (2013). Spatial-temporal variations of evapotranspiration and runoff/precipitation ratios responding to the changing climate in the Pacific Northwest during 1921–2006. *Journal of Geophysical Research-Atmospheres*, 118, 380–394.
- Livneh, B., Deems, J. S., Buma, B., Barsugli, J. J., Schneider, D., Molotch, N. P., ... Wessman, C. A. (2015). Catchment response to bark beetle outbreak and dust-on-snow in the Colorado Rocky Mountains. *Journal of Hydrology*, 523, 196–210.
- Marshall, J. D., & Waring, R. H. (1986). Comparison of methods of estimating leaf-area index in old-growth Douglas-fir. *Ecology*, 67, 975–979.
- Montesi, J., Elder, K., Schmidt, R. A., & Davis, R. E. (2004). Sublimation of intercepted snow within a subalpine forest canopy at two elevations. *Journal of Hydrometeorology*, 5, 763–773.
- Moore, R. D., & Wondzell, S. M. (2005). Physical hydrology and the effects of forest harvesting in the Pacific Northwest: A review. *Journal of the American Water Resources Association*, 41, 763–784.
- Nanko, K., Onda, Y., Kato, H., & Gomi, T. (2015). Immediate change in throughfall spatial distribution and canopy water balance after heavy thinning in a dense mature Japanese cypress plantation. *Ecohydrology*. DOI: 10.1002/eco.1636.
- Nelson, K., Kurc, S. A., John, G., Minor, R., & Barron-Gafford, G. A. (2014). Influence of snow cover duration on soil evaporation and respiration efflux in mixed-conifer ecosystems. *Ecohydrology*, 7, 869–880.
- Norby, R. J., Zak, D. R. (2011). Ecological lessons from free-air CO₂ enrichment (FACE) experiments. In: *Annual Review of Ecology, Evolution, and Systematics*, Vol 42. Annual Reviews, Palo Alto, p. 181–203.
- ORNL. (2014). Oak Ridge National Laboratory. Retrieved from: http://daac.ornl.gov/DAYMET/guides/Daymet_mosaics.html#Daymet_m_citation
- Pearce, A. J., Rowe, L. K., & Stewart, J. B. (1980). Nighttime, wet canopy evaporation rates and the water-balance of an evergreen mixed forest. *Water Resources Research*, 16, 955–959.
- Pypker, T. G., Bond, B. J., Link, T. E., Marks, D., & Unsworth, M. H. (2005). The importance of canopy structure in controlling the interception loss of rainfall: Examples from a young and an old-growth Douglas-fir forest. *Agricultural and Forest Meteorology*, 130, 113–129.
- RCP. (2015). Representative concentration pathways. Retrieved from: <http://tntcat.iiasa.ac.at/RcpDb/dsd?Action=htmlpage&page=welcome#intro>
- Rogers, B. M., Neilson, R. P., Drapek, R., Lenihan, J. M., Wells, J. R., Bachelet, D., & Law, B. E. (2011). Impacts of climate change on fire regimes and carbon stocks of the U.S. Pacific Northwest. *Journal of Geophysical Research - Biogeosciences*, 116, 13.
- Runyon, J., Waring, R. H., Goward, S. N., & Welles, J. M. (1994). Environmental limits on net primary production and light use efficiency across the Oregon transect. *Ecological Applications*, 4, 226–237.
- Rupp, D. E., Abatzoglou, J. T., Hegewisch, K. C., & Mote, P. W. (2013). Evaluation of CMIP5 20th century climate simulations for the Pacific Northwest USA. *Journal of Geophysical Research-Atmospheres*, 118, 10884–10906.
- Shafer, S. L., Bartlein, P. J., Gray, E. M., & Pelltier, R. T. (2015). Projected future vegetation changes for the northwest United States and southwest Canada at a fine spatial resolution using a dynamic global vegetation model. *PLoS One*, 10, 21.
- Shafer, S. L., Bartlein, P. J., & Thompson, R. S. (2001). Potential changes in the distributions of western North America tree and shrub taxa under future climate scenarios. *Ecosystems*, 4, 200–215.
- SNOTEL. (2016). Snow telemetry and snow course data and products. Retrieved from: <http://www.wcc.nrcs.usda.gov/snow/>
- Stoof, C. R., Vervoort, R. W., Iwema, J., van den Elsen, E., Ferreira, A. J. D., & Ritsema, C. J. (2012). Hydrological response of a small catchment burned by experimental fire. *Hydrology and Earth System Sciences*, 16, 267–285.
- Storck, P., Lettenmaier, D. P., & Bolton, S. M. (2002). Measurement of snow interception and canopy effects on snow accumulation and melt in a mountainous maritime climate, Oregon, United States. *Water Resources Research*, 38, 16.
- Tague, C., Heyn, K., & Christensen, L. (2009). Topographic controls on spatial patterns of conifer transpiration and net primary productivity under climate warming in mountain ecosystems. *Ecohydrology*, 2, 541–554.
- Tesemma, Z. K., Wei, Y., Peel, M. C., & Western, A. W. (2015). Including the dynamic relationship between climatic variables and leaf area index in a hydrological model to improve streamflow prediction under a changing climate. *Hydrology and Earth System Sciences*, 19, 2821–2836.
- Thomas, C. K., Law, B. E., Irvine, J., Martin, J. G., Pettijohn, J. C., & Davis, K. J. (2009). Seasonal hydrology explains interannual and seasonal variation in carbon and water exchange in a semi-arid mature ponderosa pine forest in central Oregon. *Journal of Geophysical Research - Biogeosciences*, 114. DOI:10.1029/2009jg001010.
- Thornton, P. E., Law, B. E., Gholz, H. L., Clark, K. L., Falge, E., Ellsworth, D. S., ... Sparks, J. P. (2002). Modeling and measuring the effects of disturbance history and climate on carbon and water budgets in evergreen needleleaf forests. *Agricultural and Forest Meteorology*, 113, 185–222.
- Tohver, I. M., Hamlet, A. F., & Lee, S. Y. (2014). Impacts of 21st-century climate change on hydrologic extremes in the Pacific Northwest region of North America. *Journal of the American Water Resources Association*, 50, 1461–1476.
- Turner, D. P., Conklin, D. R., & Bolte, J. P. (2015a). Projected climate change impacts on forest land cover and land use over the Willamette River Basin, Oregon, USA. *Climatic Change*, 133, 335–348.
- Turner, D. P., Ritts, W. D., Yang, Z. Q., Kennedy, R. E., Cohen, W. B., Duane, M. V., ... Law, B. E. (2011). Decadal trends in net ecosystem production and net ecosystem carbon balance for a regional socioecological system. *Forest Ecology and Management*, 262, 1318–1325.
- Turner, D. P., Ritts, W. D., Kennedy, R., Gray, A., & Yang, Z. (2015b). Effects of harvest, fire, and pest/pathogen disturbances on the West Cascades ecoregion carbon balance. *Carbon Balance and Management*, 10, 12.
- Unsworth, M. H., Phillips, N., Link, T., Bond, B. J., Falk, M., Harmon, M. E., ... Paw, U. K. T. (2004). Components and controls of water flux in an old-growth Douglas-fir-western hemlock ecosystem. *Ecosystems*, 7, 468–481.
- Way, D. A., Oren, R., & Kroner, Y. (2015). The space-time continuum: The effects of elevated CO₂ and temperature on trees and the importance of scaling. *Plant, Cell and Environment*, 38, 991–1007.
- Wharton, S., Schroeder, M., Bible, K., Falk, M., & Paw, K. T. (2009). Stand-level gas-exchange responses to seasonal drought in very young versus old Douglas-fir forests of the Pacific Northwest, USA. *Tree Physiology*, 29, 959–974.
- WW2100. (2015). Willamette Water 2100 Project web page, <http://water.oregonstate.edu/ww2100/>

How to cite this article: Turner, D. P., Conklin, D. R., Vache, K. B., Schwartz, C., Nolin, A. W., Chang, H., Watson, E., and Bolte, J. P. (2016), Assessing mechanisms of climate change impact on the upland forest water balance of the Willamette River Basin, Oregon, *Ecohydrology*, doi: 10.1002/eco.1776